Available online at www.sciencedirect.com
ScienceDirect
Journal of Luminescence 122-123 (2007) 967–969
JOURNAL OF LUMINESCENCE
www.elsevier.com/locate/jlumin

Optical properties of Er^{3+}-doped telluride glasses with P_2O_5 addition for 1.5 μm broadband amplifiers

Yongshi Luo[a,c], Jiahua Zhang[a,*], Shaozhe Lu[a], Xiao-jun Wang[a,b]

[a]Key Laboratory of Excited State Processes, Changchun Institute of Optics, Fine Mechanics and Physics, Chinese Academy of Sciences, 16 Eastern South Lake Road, Changchun 130033, PR China
[b]Department of Physics, Georgia Southern University, Statesboro, GA 30460, USA
[c]Graduate school of Chinese Academy of Sciences, Beijing 100039, China

Available online 15 March 2006

Abstract

In this paper, P_2O_5 has been introduced into Er^{3+}-doped telluride glasses. Emission and absorption spectra of the new glass are studied. It is observed that the nonradiative relaxation rate of $^4I_{11/2}$–$^4I_{13/2}$ transitions and the 1.5 μm emission efficiency increases with the increase in P_2O_5 content. The nonradiative relaxation rate of $^4I_{11/2}$–$^4I_{13/2}$ transition in a glass with 7 mol% P_2O_5 is four times greater than that without P_2O_5. The P_2O_5 additives can also increase the thermal stability of the telluride glass. The present results indicate that telluride glasses with P_2O_5 addition may be a promising candidate medium for broadband erbium-doped fiber amplifiers.
© 2006 Elsevier B.V. All rights reserved.

PACS: 42.70.C; 78.20.C; 81.05.Pj; 74.25.Gz

Keywords: Erbium; Telluride glasses; Nonradiative decay

1. Introduction

In recent years, Er^{3+}-doped glasses with a broad 1.5 μm emission band originating from $^4I_{13/2}$–$^4I_{15/2}$ transition of Er^{3+} have been extensively investigated for use in erbium-doped fiber amplifiers (EDFA) [1–3]. Among the reported materials, Er^{3+}-doped telluride glasses have exhibited a wide 1.5 μm emission band, a large stimulated emission section, and a high 1.5 μm emission efficiency. A telluride glass-based fiber with 76 nm flat gain bands has been reported in 1997 [4]. However, as a host for EDFA, telluride glass has some major drawbacks. One of them is the phonon energy of the glass is about 770 cm^{-1}, which leads to the $^4I_{11/2}$–$^4I_{13/2}$ nonradiative relaxation rate too slow to allow efficient pumping at 980 nm.

To overcome the drawback, co-doping Ce^{3+} was reported [5,6] to enhance the 980 nm pumping efficiency through the non radiative energy transfer. Another method was carried out introducing B_2O_3 [6], which has a large phonon energy of B–O bond, resulting in the increase of the pumping efficiency at 980 nm through multi-phonon relaxation. In such a system, however, the multi-phonon relaxation rate of $^4I_{13/2}$–$^4I_{15/2}$ transition of Er^{3+} is also speeded up, leading to an obvious decrease of the 1.5 μm emission efficiency, so it is not suitable for application.

In this paper, we report the effect of P_2O_5 content on the optical and thermal properties of the Er^{3+}-doped tungsten–telluride glass. $^4I_{11/2}$–$^4I_{13/2}$ nonradiative transition as well as $^4I_{11/2}$–$^4I_{15/2}$ (0.98 μm) and $^4I_{13/2}$–$^4I_{15/2}$ (1.5 μm) radiative transitions are studied.

2. Experimental

Er^{3+}-doped glasses, $(40-0.4x)TeO_2$–$(30-0.3x)WO_3$–$(30-0.3x)Li_2O$–xP_2O_5 ($x = 0,1,2,3,4,5,7$) (TWP for series, and TWxP, where $x = 0,1,2,3,4,5,7$, for individual glass) and $70TeO_2$–$20ZnO$–$10Na_2O$ (TZN glass) doped with Er^{3+} at a constant concentration of 1.0 mol% were prepared using the conventional melting and quenching method. Well-mixed powder in a crucible was allowed to melt at 750–850 °C for 1 h, and then was quenched into a

*Corresponding author. Tel.: +86 431 617 6317; fax: +86 431 617 6317.
E-mail address: zjiahua@public.cc.jl.cn (J. Zhang).

0022-2313/$ - see front matter © 2006 Elsevier B.V. All rights reserved.
doi:10.1016/j.jlumin.2006.01.340

preheated brass mold to form glass. The quenched sample was annealed around the glass transition temporarily for 2 h and then cooled inside the furnace down to room temperature. The obtained glass samples were cut and polished into $10 \times 10 \times 2.0\,mm^3$ sized pieces.

Emission spectra in the range of 900–1700 nm were measured using a TRIAX-550 spectrometer under excitation of 808 nm from a laser diode. Absorption spectra were measured using a UV-3101PC spectrometer. The lifetime of the $^4I_{13/2}$ state for Er^{3+} was measured with a 500 MHz Tektronix digital oscilloscope under excitation of 808 nm light pulses from an optical parametric oscillator. The differential thermal analysis (DTA) data was collected using a Perkin–Elmer 7 Series Thermal Analysis System. All the measurements were taken at room temperature.

3. Results and discussion

3.1. Infrared emission spectra of Er^{3+}

Fig. 1 shows the infrared emission spectra of Er^{3+} in the range 800–1700 nm in TWP samples. The value of full-width at half-maximum (FWHM) at 1.5 μm emission is about 65 nm, which is not affected with additional composition of P_2O_5. It can be seen that the ratio of the integrated intensity of the 1.5 μm band to that of the 0.98 μm (denoted as α in Section 3.3 and listed in Table 1.) increases as P_2O_5 content increases, as shown in Fig. 1. This ratio is mainly governed by $^4I_{11/2}$–$^4I_{13/2}$ nonradiative relaxation rate. It suggests that $^4I_{11/2}$–$^4I_{13/2}$ nonradiative relaxation rate increases with the increase of P_2O_5, which may modify the phonon energies of the glass.

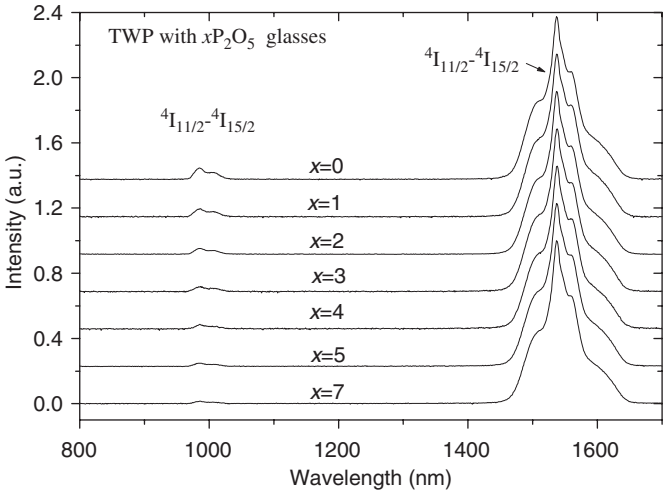

Fig. 1. Emission spectra from $^4I_{11/2}$–$^4I_{15/2}$ and $^4I_{13/2}$–$^4I_{15/2}$ transitions of Er^{3+} in $(40-0.4x)TeO_2$–$(30-0.3x)WO_3$–$(30-0.3x)Li_2O$–xP_2O_5 (x = 0,1,2,3,4,5,7) glasses. Emission intensities are normalized to the $^4I_{13/2}$–$^4I_{15/2}$ transition.

3.2. The $^4I_{13/2}$ lifetime

Lifetimes of $^4I_{13/2}$ level (τ_1) of Er^{3+} in TWP glass are measured and listed in Table 1. It can be seen that the lifetime of the $^4I_{13/2}$ state increases from 3.3 to 4 ms with the increase of the P_2O_5 content up to 7 mol%, while the radiative lifetime τ_{1r} obtained from Judd–Ofelt analysis of the absorption spectra are almost unchanged, leading to the increase of 1.5 μm emission efficiency η_1, as shown in Table 1.

3.3. The $^4I_{11/2}$-$^4I_{13/2}$ nonradiative relaxation rates

Fig. 2 depicts an energy level diagram of Er^{3+} at low energy levels. When pumped by 808 nm laser diode, Er^{3+} is excited from ground state to $^4I_{9/2}$ level, which rapidly relaxes to $^4I_{11/2}$ state through nonradiative decay. Subsequently, the $^4I_{13/2}$ level is populated. The rate of $^4I_{11/2}$–$^4I_{13/2}$ relaxation is very important for creating population inversion of $^4I_{13/2}$ level for optical amplification at 1.5 μm. In the steady excitation, for $^4I_{11/2}$ state, one has

$$A_{21}n_2 + W_{21}n_2 = n_1/\tau_1, \tag{1}$$

where A_{21} is $^4I_{11/2}$–$^4I_{13/2}$ radiative transition rate, W_{21} is $^4I_{11/2}$–$^4I_{13/2}$ nonradiative relaxation rate, n_2 and n_1 are the populations of the $^4I_{11/2}$ and $^4I_{13/2}$ levels respectively. Letting α be the measured ratio of the 1.5 μm emission intensity to that of the 0.98 μm, we have

$$\alpha = CA_{10}n_1/A_{20}n_2, \tag{2}$$

where C is a calibration coefficient related to measurement device only. From Eqs. (1) and (2), we have

$$W_{21} = \alpha A_{20}/CA_{10}\tau_1 - A_{21}, \tag{3}$$

Table 1
Measured lifetime of Er^{3+}-adopted $^4I_{13/2}$ level (τ_1), radiative transition rates (A_{10} and A_{20}) calculated from the absorption spectra and measured intensity ratio $\tilde{\alpha}$

Glass	τ_{1r} (ms) $^4I_{13/2}$	τ_1 (ms) $^4I_{13/2}$	η_1 (%) $^4I_{13/2}$	A_{10} (s^{-1}) $^4I_{13/2}$-$^4I_{15/2}$	A_{20} (s^{-1}) $^4I_{11/2}$-$^4I_{15/2}$	α
TW0P	4.11	3.3	80	243.18	333.56	28.7
TW1P	3.963.96	3.3	83	252.37	346.91346.91	37.7
TW2P	4.114.11	3.3	80	243.27	330.80330.8	55.4
TW3P	4.22	3.3	78	237.11	323.24	60.1
TW4P	4.124.12	3.4	82	242.85	334.83334.83	76.9
TW5P	4.23	3.7	87	236.54236.57	323.35	94.7
TW7P	4.27	4.2	98	233.97	321.54	135.5
TZN	4.5	3.67	81	220.20	304.51	21.1

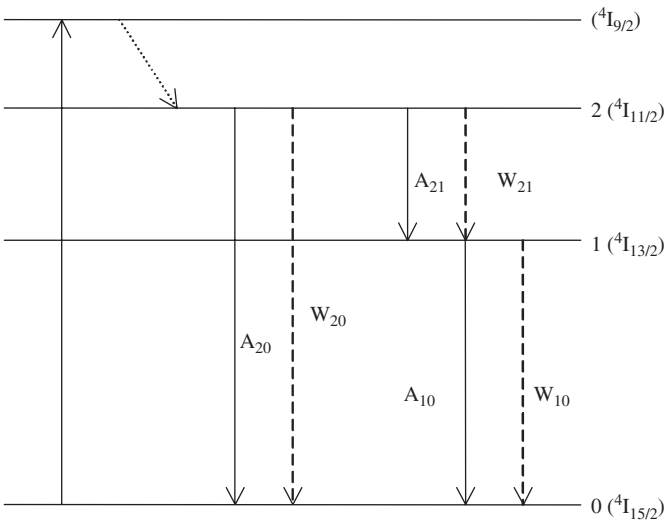

Fig. 2. An energy level diagram of Er^{3+} ions. The transition from $^4I_{15/2}$–$^4I_{11/2}$ indicates an optical transition under 980 nm excitation. Solid lines represent the radiative processes and dashed lines are the nonradiative processes.

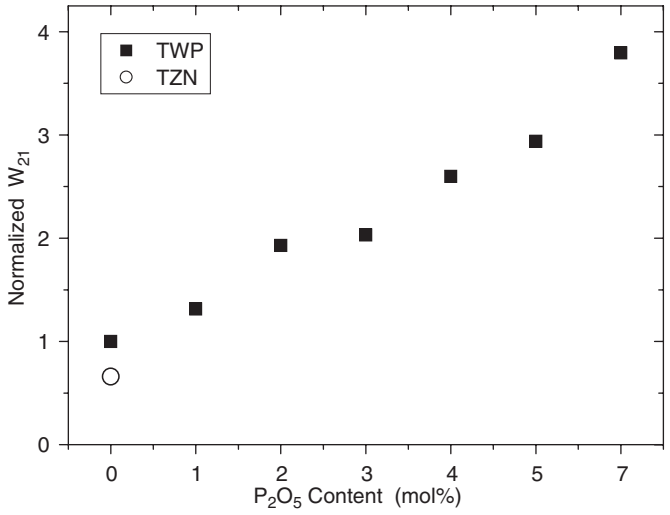

Fig. 3. The $^4I_{11/2}$–$^4I_{13/2}$ nonradiative relaxation rates for various P_2O_5 contents in TWP glasses. The rates (W_{21}) for TWP glass (squares) and TZN glass (circle) are normalized, respectively, to the rate of TW0P glass.

where A_{21} can be neglected because $W_{21} \gg A_{21}$. Hence, we obtain

$$W_{21}/W_{21}(0) = \alpha A_{20}A_{10}(0)\tau_1(0)/\alpha(0)A_{20}(0)A_{10}\tau_1, \quad (4)$$

where $W_{21}(0)$, $A_{10}(0)$, $A_{20}(0)$ and $\alpha(0)$ are the parameters corresponding to the TW0P glass. According to the Judd–Ofelt theory [7,8], A_{20} and A_{10} are calculated from the measured absorption spectra and listed in the Table 1. Using Eq. (4), W_{21} values with the unit of $W_{21}(0)$ are then calculated and plotted in Fig. 3.

As indicated in Fig. 3, W_{21} increases with the increase of P_2O_5 content, which has large phonon energy of P–O bond, resulting in the increased multi-phonon relaxation between $^4I_{11/2}$ and $I_{13/2}$ levels of Er^{3+}. The nonradiative relaxation rate of the $^4I_{11/2}$–$^4I_{13/2}$ transition in a glass with 7 mol% P_2O_5 is about four times higher than that in a glass without P_2O_5, and is about 6 times higher than that in TZN glass, which is also indicated in Fig. 3. Obviously, under 0.98 μm pumping, feeding of $^4I_{13/2}$ of Er^{3+} in TWP glass is more efficient than that in TZN glass.

3.4. Thermal stability of TWP glass

Differential thermal analysis trace of the TW5P sample at a heat rate of 600 °C/h has been done. The difference between the glass transition temperature (T_g) and the onset crystallization temperature (T_x), $\Delta T = T_x - T_g$, has been frequently used as a rough estimate of glass formation ability or glass thermal stability. To avoid crystallization during fiber drawing, it is desirable for a glass host to have as large a ΔT as possible. In our experiment, T_g is about 386 °C and T_x is about 567 °C, and the temperature difference ΔT of the glasses is above 180 °C, which is greater than 125 °C, the temperature difference for a tungsten–telluride glass without P_2O_5 composition [9], indicating that the TW5P glass has better thermal stability.

4. Conclusions

Adding P_2O_5 into Er^{3+}-doped telluride glasses can increase both the nonradiative relaxation rate of the $^4I_{11/2}$–$^4I_{13/2}$ transition and the 1.5 μm emission efficiency. The nonradiative relaxation rate of $^4I_{11/2}$–$^4I_{13/2}$ transition of the TWP glass with 7 mol% P_2O_5 is about four times higher than that in a glass without P_2O_5, indicating an obvious improvement of population feeding efficiency of $^4I_{13/2}$ from $^4I_{11/2}$ level pumped at 980 nm. The P_2O_5 additives can also increase the thermal stability of the telluride glass. The present results indicate that telluride glasses with P_2O_5 addition may be a promising candidate medium for broadband erbium-doped fiber amplifiers.

Acknowledgments

The authors acknowledge the supports by MOST of China (No. 2006CB601104), the National Natural Foundation of China under grant no. 90201010 and One Hundred Talents Program of Chinese Academy of Sciences.

References

[1] J.S. Wang, E.M. Vogel, E. Snitzer, Opt. Mater. 3 (1994) 187.
[2] S. Tanabe, N. Sugimoto, S. Ito, T. Hanada, J. Lumin. 87–89 (2000) 670.
[3] X. Feng, S. Tanabe, T. Hanada, J. Am. Ceram. Soc. 84 (2001) 165.
[4] A. Mori, Y. Ohishi, S. Sudo, Electron. Lett. 33 (1997) 863.
[5] S. Shen, M. Naftaly, A. Jha, Opt. Commun. 205 (2002) 101.
[6] D.H. Cho, Y.G. Choi, K.H. Kim, ETRI J. 23 (2001) 151.
[7] B.R. Judd, Phys. Rev. 127 (1962) 750.
[8] G.S. Ofelt, J. Chem. Phys. 37 (1962) 511.
[9] X. Feng, C. Qi, F. Lin, H. Hu, J. Non-Cryst. Solids 256–257 (1999) 372.